(Authors)

Masataka Nakayama[a], Shihomi Imamura[a], Chikae Tatsumi[a,b], Takeshi Taniguchi[c], Ryunosuke Tateno[d]

(Title)

Microbial functions and soil nitrogen mineralisation processes in the soil of a cool temperate forest in northern Japan

(The affiliations of the authors)

[a] *Graduate School of Agriculture, Kyoto University, Kyoto 606-8502, Japan*

[b] *Research Faculty of Agriculture, Hokkaido University, Hokkaido, 060-8589, Japan*

[c] *Arid Land Research Center, Tottori University, Tottori 680-0001, Japan*

[d] *Filed Science Education and Research Center, Kyoto University, Kyoto 606-8502, Japan*

(Corresponding Author)

Masataka Nakayama

Graduate School of Agriculture, Kyoto University, Kyoto 606-8502, Japan

Tel: +81-75-753-6440, Fax: +81-75-753-6443

E-mail: nakayama.masataka.32x@st.kyoto-u.ac.jp

(ORCID)

Masataka Nakayama: 0000-0003-3835-5512

Chikae Tatsumi: 0000-0001-7191-6049

Takeshi Taniguchi: 0000-0001-7386-1117

Ryunosuke Tateno: 0000-0001-8461-3696

Abstract

There is little knowledge about microbial functional community structures and the relationships between microbial communities and nitrogen transformation processes. Here, we investigated the relationships between soil microbial communities and nitrogen mineralisation potentials in a cool temperate forest throughout the growing season. Microbial communities were assessed by quantification of the total bacterial, archaeal, and fungal gene abundances and the bacterial and archaeal amoA gene abundances, functional predictions of bacteria and fungi, and analysis of the bacterial-fungal co-occurrence network. In mid-summer, ectomycorrhizal fungal abundance was significantly higher, whereas the total bacterial abundance was significantly lower. Bacterial and archaeal amoA gene abundances were also significantly higher in mid-summer. However, regardless of the seasonal fluctuation of microbial gene abundances, the net nitrification and nitrogen mineralisation potential did not show clear seasonality. In the network analysis, the microbial community was divided into 13 modules, which were subgroups assumed to have similar niches. Furthermore, two modules that mainly consisted of microbial species of Proteobacteria and Bacteroidetes were significantly and positively correlated with the net nitrification and mineralisation potentials. Our results indicated that microbial subgroups sharing similar niches, instead of total microbial abundances and functional gene abundances, could be important factors affecting the net nitrogen mineralisation potential.

Keywords

Soil microbial community, co-occurrence network, modules, nitrogen cycle

Declarations

Funding

This study was supported by JSPS-KAKENHI: 18H02241, 26292085, 23780166

Conflict of interest

The authors declare that they have no conflict of interest.

Availability of data and material

The datasets generated during and/or analysed during the current study are available from the corresponding author on reasonable request.

Code availability

Not applicable

Authors' contribution

MN, SI and RT conceived and designed the experiment; MN, SI and RT performed the experiment; MN, SI, CT and TT performed data analysis; MN prepared figures and tables; MN and RT took the lead in writing the manuscript with input from all authors.

Acknowledgements

We would like to thank Dr. Takahito Yoshioka, Dr. Kazuya Kobayashi and the member of Forest Information Laboratory for the helpful suggestion. We also thank Takayuki Yamauchi, Yasuyuki Shibata, Tomoyuki Nakagawa, Jun Yanagimoto, Ken-ichi Ohta, Yuhei Nishioka, Makoto Furuta, Yasunori Kishimoto, Yoichiro Kitagawa, Masaru Okuda, Akira Yamanaka, Yuta Miyagi, Syuichi Sato, Yukie Kawamura and Michiko Shimizu as the staffs of Hokkaido forest research station, Field Science Education and Research Center, Kyoto University for helping the experiments. This study was supported by JSPS-KAKENHI (No. 23780166, 26292085, 18H02241).

Introduction

The availability of nitrogen (N) often limits the primary production of temperate forests (Vitousek and Howarth, 1991; LeBauer and Treseder, 2008). Nitrogen mineralisation and nitrification, wherein organic N is converted into plant-available N forms, are the key processes regulating aboveground and belowground net primary production and N cycling in forest ecosystems (Aber *et al.*, 1985; Reich *et al.*, 1997; Tateno *et al.*, 2004). Soil microbial communities, including fungi and bacteria, are thought to be the main drivers of soil N transformation processes (Schimel and Bennett, 2004; Isobe and Ohte, 2014; Tatsumi *et al.*, 2019; Isobe *et al.*, 2020). Therefore, to understand the forest soil N cycle, it is essential to understand soil microbial communities.

In the last two decades, studies have revealed that microbial abundances, communities, and functional gene abundances are affected by environmental conditions including pH, carbon/nitrogen (C/N) ratio, and availability of nutrients and substrates (Högberg *et al.*, 2007; Lauber *et al.*, 2008; Ushio *et al.*, 2010; Wan *et al.*, 2015). Therefore, soil microbial communities can respond to changes in environmental conditions caused by seasons and/or tree species composition of the forests (Moore-Kucera and Dick, 2008; Ushio *et al.*, 2010; Prevost-Boure *et al.*, 2011). Individual tree species also affect soil microbial communities directly by organic carbon supply from their roots (Kaiser *et al.*, 2010, 2011; Urbanová *et al.*, 2015), which can change between seasons and/or with the tree species composition of forests. In particular, mycorrhizal fungi rely on the carbon supply from their symbiotic trees (Gessler *et al.*, 1998; Högberg *et al.*, 2010; Ekblad *et al.*, 2013), which can affect the free-living microbial community that is involved in soil N transformation processes (Tatsumi *et al.*, 2020).

Furthermore, relationships between microbial communities and soil N transformation processes have been reported in earlier studies (Boyle *et al.*, 2008; Gubry-Rangin *et al.*, 2010; Isobe

106 *et al.*, 2015, 2020; Ribbons *et al.*, 2016; Tatsumi *et al.*, 2020). For example, Ribbons *et al.* (2016)
107 found that the total bacterial abundance had a positive and significant correlation with N
108 mineralisation rates. In addition, rare bacterial and archaeal groups sometimes have significant roles
109 in specific processes (Caffrey *et al.*, 2007; Isobe and Ohte, 2014; Isobe *et al.*, 2020). For example,
110 the abundance of ammonia-oxidising bacteria and archaea (AOB and AOA, respectively) affected
111 the nitrification rate (Isobe *et al.*, 2015, 2020; Ribbons *et al.*, 2016). However, since microbial
112 functions and metabolisms have high diversities (Torsvik and Øvreås, 2002; Strickland *et al.*, 2009;
113 Mendes *et al.*, 2014; Lladó *et al.*, 2016; Wilhelm *et al.*, 2019), the underlying mechanisms by which
114 microbial communities drive N transformation processes are still largely unknown.

115 Recently, the microbial co-occurrence network analysis has provided new insights for
116 understanding microbial communities (Toju *et al.*, 2016; Sun *et al.*, 2017; Nakayama *et al.*, 2019). It
117 has detected densely co-occurring microbial subgroups, called modules (Newman, 2006; Langfelder
118 and Horvath, 2008; Deng et al., 2012), and the analyses of these modules could be used to uncover
119 ecologically relevant interactions that could not be detected by the traditional analyses of community
120 compositions and abundances. Although it is difficult to detect which co-occurring relationships
121 could be a direct physical interaction or an apparent co-occurrence, the microbial subgroups detected
122 as modules would have an individual preference for substrates and environmental conditions (Deng
123 *et al.*, 2012; de Menezes *et al.*, 2015; Jones and Hallin, 2019). Highlighting the microbial modular
124 subgroups would allow for a detailed investigation of the microbial communities that could not be
125 achieved by analysing the whole microbial community (de Menezes *et al.*, 2015). For example,
126 Purahong *et al*. (2016) reported that individual fungal sub-communities detected as modules had
127 different preferences for the chemical compositions of leaf litter, and only a part of the detected
128 modules had significant roles in litter degradation. Thus, investigating the relationships between
129 modular microbial subgroups and N mineralisation processes would reveal the detailed mechanisms

of microbial regulation for soil N transformation.

Recently, we investigated the impact of conversion of a forest to a monoculture plantation on the characteristics of microbial communities, such as the diversities and co-occurrence network structures of the communities. We found that forest conversion reduced the robustness of the co-occurrence network in mineral soil, while microbial diversities were maintained (Nakayama *et al.*, 2019). We also reported that chemical properties, including pH and the C/N ratio, significantly varied among seasons but not among forest types (Nakayama *et al.*, 2019). However, the details of the interactions between each functional group of the microbial communities and the N mineralisation processes are still unknown. Therefore, in the current study, we aimed to reveal the relationships between the roles of each group of microbial communities and the N transformation processes in the soil of a cool temperate forest. We measured the net nitrification and N mineralisation potentials, total gene abundances of bacteria, archaea, and fungi, and the bacterial and archaeal *amoA* gene abundances among forest types (monoculture larch and fir plantations, and natural deciduous broad-leaved forests) and months (May, July, August, September, and November). Furthermore, we predicted the bacterial functional gene abundances, fungal guilds, and trophic modes by using the sequencing results reported previously (Nakayama *et al.*, 2019). Moreover, a microbial co-occurrence network was constructed and the microbial community was divided into modules. We then analysed the relationships between the microbial modules and the net N transformation processes. We hypothesised that: (1) microbial abundance and functional communities change due to the differences in seasons and/or forest types, (2) differences in microbial abundance and functional communities regulate changes in the N transformation processes, (3) individual modules in the co-occurrence network each have relationships with N mineralisation and nitrification potentials, and (4) modules that fluctuate with differences in seasons and forest types are particularly important for the N mineralisation and nitrification potentials.

Materials and Methods

Study site and soil sampling

We conducted this study in cool-temperate deciduous broad-leaved natural forests (hereafter referred to as “Natural”) and two kinds of plantations (“Larch” and “Fir”) that were converted from natural forests in the Shibecha Branch of the Hokkaido Forest Research Station at the Field Science Education and Research Center, Kyoto University, in north-east Japan (43°24.2′N, 144°38.5′E). The mean annual precipitation and air temperature were 1,189 mm and 6.3℃ (1986–2015), respectively. The highest average air and soil temperatures were usually observed in August, while leaves fell from deciduous trees in October (Nakayama and Tateno, 2018). The soils at this site were characterised as andosols (IUSS Working Group WRB, 2015).

Natural forests were typically dominated by *Quercus crispula* Blume, *Ulmus davidiana* var. *japonica* Nakai, *Phellodendron amurense* Rupr., *Acer pictum* Thunb. subsp. mono (Maxim.) H. Ohashi, and *Fraxinus mandshurica* Rupr. var. *japonica*, and the forest floor was densely covered with *Sasa nipponica* Makino et Shibata. The Larch and Fir plantations were plantations of *Larix kaempferi* (Lamb.) Carr. and *Abies sachalinensis* (Shmidt) Masters, respectively. We established four plots in each of the three forest types (Natural, Larch, and Fir) for soil sampling. The dominant trees of all the forest types were ectomycorrhizal trees (Matsuoka *et al.*, 2020). On May 29, July 15, August 26, September 17, and November 9, 2012, five surface mineral soil cores (0–10 cm depth) were collected using a cylindrical soil core sampler (20 cm^2 in surface area) from each plot and composited. The details of sampling plots and soil sampling have been reported previously (Nakayama *et al.*, 2019).

178 The samples were sieved with a 4 mm mesh sieve and divided into subsamples for wet,
179 fumigation, oven dry, and frozen treatments. The chemical properties (pH, moisture content,
180 microbial biomass C and N, total C and N, and the concentrations of dissolved organic C, NO_3^--N,
181 NH_4^+-N, dissolved inorganic N, amino acid, and dissolved organic N) of the wet and oven-dry
182 samples were previously reported (Nakayama *et al.*, 2019) and summarised in Supplementary Table
183 1. Briefly, the investigated chemical properties except for the C/N ratio significantly differed
184 between sampling months. For example, average pH ranged from 4.5 to 5.6 and was significantly
185 lower in August (Supplementary Table 1; means ± standard deviations; 4.5 ± 0.2, 4.8 ± 0.2, and 4.5 ±
186 0.4 for Larch, Fir, and Natural, respectively). There were no significant differences in other chemical
187 properties except for the microbial biomass of C and N among the forest types, which were
188 significantly higher in Natural than Fir (Supplementary Table 1).
189 DNA was also extracted from frozen subsamples (stored at −20°C) using a DNA extraction
190 kit (DNeasy Power Soil Kit, QIAGEN, Hilden, Germany), sequenced by the Ion Personal Genome
191 Machine™ (PGM™) with the Ion 318™ Chip V2 (Thermo Fisher Scientific, Waltham, MA, USA)
192 and the sequence data were processed. Detailed methods and results of the chemical properties, DNA
193 extraction and sequencing are shown in a previous report (Nakayama *et al.*, 2019), and the sequence
194 data were deposited in the DDBJ Sequence Read Archive under accession number DRA007965.
195
196 *Net nitrification and mineralisation potentials*
197
198 Wet subsamples (30 g) were put in plastic bottles and aerobically incubated for one month at 25°C.
199 To maintain the soil moisture at initial values, ion-exchanged water was added every ten days. After
200 the incubation period, ten grams of each subsample were extracted in 100 ml of 0.5 M K_2SO_4
201 solution. The net nitrification and mineralisation potentials were calculated as the net increase in the

amount of NO_3^--N and the total inorganic N over the incubation period, respectively. The initial values of NH_4^+-N and NO_3^--N were reported by Nakayama et al. (2019).

Microbial gene quantifications and functional predictions

Microbial gene abundance was quantified by the real-time quantitative polymerase chain reaction (qPCR) performed by the LightCycler 96 System (Roche Diagnostics K.K., Mannheim, Germany), with an intercalating dye, SYBR Green I (FastStart Essential DNA Green Master, Roche Diagnostics K.K., Mannheim, Germany). The bacterial and archaeal 16S rRNA genes, fungal ITS regions of the rRNA genes, and the bacterial and archaeal ammonia monooxygenase genes (*amoA*) were quantified to estimate total bacteria, total archaea, total fungi, AOB and AOA, respectively. The bacterial 16S, archaeal 16S, fungal ITS, bacterial *amoA*, and archaeal *amoA* were determined using universal primer sets 338f (Amann *et al.*, 1990)/518r (Muyzer *et al.*, 1993), 109f (Großkopf *et al.*, 1998)/344r (Raskin *et al.*, 1994), ITS1F_KYO2/ITS2_KYO2 (Toju *et al.*, 2012), amoA 1F/amoA 2R (Rotthauwe *et al.*, 1997), and CrenamoA 23F/CrenamoA 616R (Tourna *et al.*, 2008), respectively. The amplifications of bacterial and archaeal 16S and fungal ITS were performed under the following conditions: an initial denaturation at 95℃ for 10 min, followed by 45 cycles at 95℃ for 1 min, 53℃ for 30 s and 72℃ for 1 min (Fierer *et al.*, 2005). The amplification of bacterial and archaeal *amoA* was performed under the following conditions: an initial denaturation at 95℃ for 10 min, followed by 45 cycles of 95℃ for 1 min, 55℃ (for bacterial *amoA*) or 52℃ (for archaeal *amoA*) for 30 s, and 72℃ for 30 s (Okano *et al.*, 2004). More details are described in previous reports (Iwaoka *et al.*, 2018; Tatsumi *et al.*, 2019).

The bacterial functional genes and the fungal trophic modes and guilds were predicted by using PICRUSt pipeline (Langille *et al.*, 2013) and FUNGuild database (Nguyen *et al.*, 2016) based

on previously published rarefied data of mineral soil 16S rRNA gene sequences and the fungal taxonomic data of the ITS sequence of the samples (Nakayama *et al.*, 2019), respectively. The number of rarefied sequence reads per sample was 1441 for the 16S rRNA gene and 5817 for the ITS region (Nakayama *et al*., 2019). This corresponded to 1170 bacterial OTUs (186 ± 18 per sample) and 2288 fungal OTUs (99 ± 26 per sample). The estimated counts of genes by PICRUSt were tagged with the KEGG Orthology (Kanehisa *et al.*, 2016). The occurrence of the genes encoding enzymes for N degradation and mineralisation, chitinase (EC 3.2.1.14), N-acetylglucosaminidase (NAGase, EC3.2.1.52), leucine aminopeptidase (EC 3.4.11.1), arginase (EC 3.5.3.1), and urease (EC 3.5.1.5) were predicted from the counts of K01183, K01207, K01255, K01476, and K01428, respectively (Isobe *et al*., 2018; Tatsumi *et al*., 2020). The activities and genes abundance of these enzymes are commonly measured to evaluate forest soil N cycling (e.g. Saiya-Cork *et al*., 2002; Sinsabaugh *et al*., 2008; Isobe *et al*., 2018; Tatsumi *et al*., 2020). Furthermore, to test the enzymatic interactions in the network, the occurrences of genes encoding the enzymes involved in nitrification, ammonia monooxygenase (K10944, K10945, K10946), hydroxylamine dehydrogenase (K10535), and nitrite oxidoreductase (K00370, K00371) were predicted by PICRUSt for each OTU occurring in the network. The fungal trophic modes (e.g. saprotroph, symbiotroph) and the guilds within the symbiotrophic fungi (e.g. ectomycorrhiza, arbuscular mycorrhiza, endophyte, lichenised) were predicted by using the online application FUNGuild (Nguyen *et al.*, 2016). FUNGuild frequently predicts multiple trophic modes for a single OTU, such as Pathotroph-Saprotroph, which we then designated to the “Others” category.

The microbial co-occurrence network and module level correlation analysis

The soil microbial co-occurrence network was constructed by using the same rarefied soil bacterial

and fungal sequencing data as functional prediction (1441 and 5817 reads per sample, respectively) that was previously published in Nakayama *et al.* (2019). Because the numbers of bacterial and fungal sequence reads were not enough to analyse the rare OTUs, we mainly focused on the core and abundant microbial community in the network analysis. Our previous study aimed to reveal the difference in network structures among forest types (Nakayama *et al.*, 2019); however, this study tried to explore the relationships between the modules of the microbial co-occurrence network and N cycling processes. Therefore, we reconstructed the mineral soil co-occurrence network using all of the microbial sequencing data of the mineral soil instead of dividing it by forest types. Before the construction of the network, the abundance data for rarefied soil bacteria and fungi were mixed into one dataset to analyse bacterial-bacterial, fungal-fungal, and bacterial-fungal relationships. In total, there were 12 plots (4 plots for each 3 forest types) and 5 sampling dates (n = 60). The network construction and module detection followed our previous paper (Nakayama *et al.*, 2019). Briefly, we removed very rare OTUs occurring in less than 1/3 of samples (i.e. less than 20 samples) before the network construction to avoid the network being too complex, enhancing the determination of the core microbial community (Barberán *et al.,* 2012). After this elimination, 190 and 33 OTUs remained for bacteria and fungi, respectively. Spearman's rank correlations were calculated with all remaining OTU pairs, and *p*-values were processed based on the false discovery rate. When the correlation coefficient ρ and *q*-value of the OTU pairs were > 0.6 and < 0.001, respectively, we considered that there was a significant positive co-occurrence relationship between the OTU pair (Chao *et al.*, 2016). The OTUs that had at least one significant co-occurrence relationship with other OTUs occurred in the network as nodes. The network was visualised using the software package Gephi (ver. 0.9.2) (Bastian *et al.*, 2009). Modules in the microbial co-occurrence network were detected based on the fast greedy modularity optimisation algorithm (Clauset *et al.*, 2004).

The relationships between modules and factors (chemical properties, N mineralisation

potentials, sampling month, and forest type) were assessed by correlation analysis (Deng *et al.*, 2012). Briefly, the relative abundance matrix was divided per module and the relative abundances of each OTU was standardised to mean 0 and variance 1. The module eigenvectors were calculated by singular value decomposition following a previous study (Langfelder and Horvath, 2007). The sign of each module eigenvector was fixed by assigning a positive correlation with the average relative abundances across OTUs within modules (Langfelder and Horvath, 2007). We then analysed the Pearson correlation coefficients between the module eigenvalues and factors as the correlations between modules and factors. Categorical factors (sampling month and forest type) were converted as 0 or 1 dummy vectors before analysis. We chose a significance level of $p < 0.05$. We also tested the relationships between the estimated absolute abundances of modules and factors after multiplying each relative abundance by the total bacterial 16S rRNA and total fungal ITS gene abundance.

Statistical analysis

We used a two-way split-plot factorial analysis of variance (ANOVA) followed by Tukey's honestly significant difference test to examine the differences in the net nitrification and mineralisation potentials, the total bacterial, archaeal and fungal gene abundance, the bacterial and archaeal *amoA* gene abundance, the predicted bacterial functional gene abundance, and the fungal trophic modes and guilds among forest types (Larch, Fir, and Natural), and sampling months (May, July, August, September, and November). The correlations between microbial gene abundances and chemical properties were assessed using Pearson’s correlation analysis. We chose a significance level of $p < 0.05$ for all statistical analyses. All statistical analyses were conducted using R software (version 3.5.0).

298

299 **Results**

300

301 *Changes in net N transformation potentials*

302

303 Net N mineralisation and nitrification were temporally stable (Fig. 1; two-way ANOVA: $F = 0.69$
304 and $p = 0.607$, and $F = 0.63$ and $p = 0.643$, respectively). Net nitrification did not significantly differ
305 among forest type (Fig. 1a; two-way ANOVA: $F = 4.01$ and $p = 0.057$), while natural forest had
306 significantly higher values of net mineralisation potentials throughout all sampling months (Fig. 1b;
307 two-way ANOVA: $F = 12.98$ and $p < 0.002$). The interaction effects of sampling month and forest
308 type on net nitrification and mineralisation were not significant (Fig. 1; two-way ANOVA: $F = 0.76$
309 and $p = 0.644$, and $F = 1.22$ and $p = 0.317$, respectively).

310

311 *Changes in microbial gene abundance*

312

313 There were significant effects of the sampling month on total bacterial and archaeal 16S rRNA gene
314 abundances (two-way ANOVA: $F = 25.58$ and $p < 0.001$, and $F = 22.41$ and $p < 0.001$, respectively).
315 According to Tukey's honestly significant difference test, bacterial abundance was significantly
316 lower in August, while archaeal abundance was higher in August for all three forest types (Fig. 2a, b).
317 Total fungal ITS gene abundance did not differ significantly among sampling months (Fig. 2c;
318 two-way ANOVA: $F = 1.02$ and $p = 0.409$). The total bacterial, archaeal, and fungal gene
319 abundances were similar among the forest types regardless of sampling months (Fig. 2a, b, c;
320 two-way ANOVA: $F = 1.75$. and $p = 0.228$, $F = 2.80$ and $p = 0.114$, and $F = 0.75$ and $p = 0.500$,
321 respectively).

322 Bacterial and archaeal *amoA* gene abundances differed significantly among sampling
323 months (two-way ANOVA: $F = 8.84$ and $p < 0.001$, and $F = 15.04$ and $p < 0.001$, respectively).
324 Archaeal *amoA* gene abundance had a similar trend with archaeal 16S rRNA gene abundance, while
325 bacterial *amoA* gene abundance had the opposite trend of bacterial 16S rRNA gene abundance, i.e.
326 the abundances of bacterial and archaeal *amoA* gene were significantly higher in August than in
327 other months for all the forest types (Fig. 2d, e). Bacterial and archaeal *amoA* genes did not
328 significantly vary among the forest types (Fig. 2d, e; two-way ANOVA: $F = 0.17$ and $p = 0.844$, and
329 $F = 1.02$ and $p = 0.400$, respectively).
330 There were some significant positive and negative correlations between total bacterial,
331 archaeal, and fungal gene abundances and chemical properties such as pH, moisture content, and the
332 C/N ratio (Supplementary Table 2). Among these relationships, only the pH was positively correlated
333 with bacterial 16S gene abundance (Supplementary Table 2; $R^2 = 0.08$ and $p < 0.05$). In contrast to
334 the bacterial abundance, pH was negatively correlated with archaeal and fungal gene abundances
335 (Supplementary Table 2; $R^2 = 0.31$ and $p < 0.001$, and $R^2 = 0.11$ and $p < 0.01$, respectively). The C/N
336 ratio had a positive and the strongest relationship with fungal ITS gene abundance (Supplementary
337 Table 2; $R^2 = 0.35$ and $p < 0.001$). There were no significant relationships between the total
338 microbial gene abundances and N mineralisation potentials (Supplementary Table 2). Bacterial and
339 archaeal *amoA* genes were also significantly correlated with chemical properties such as pH and
340 dissolved organic N content (Supplementary Table 2). Bacterial and archaeal gene abundances were
341 not correlated with the nitrification and mineralisation potentials (Supplementary Table 2).
342
343 *Changes in bacterial predicted functional gene and fungal trophic modes and guilds*
344
345 Among the predicted functional genes (the genes encoding N degrading and mineralising enzymes:

chitinase, NAGase, leucine aminopeptidase, arginase, and urease), there were no significant effects of forest type (Fig. 3; two-way ANOVA: $F = 0.05$ and $p = 0.949$, $F = 0.54$ and $p = 0.601$, $F = 0.15$ and $p = 0.867$, $F = 0.02$ and $p = 0.985$, and $F = 0.37$ and $p = 0.700$, respectively) and sampling month, except for urease (Fig. 3; two-way ANOVA: $F = 2.36$ and $p = 0.072$, $F = 0.42$ and $p = 0.795$, $F = 1.19$ and $p = 0.332$, $F = 1.80$ and $p = 0.150$, and $F = 5.03$ and $p < 0.01$, respectively) on their relative abundance. The relative abundance of urease in August was significantly higher than that in May, September, and November (Fig. 3e). The estimated absolute abundances of the predicted functional genes were temporarily changed, reflecting the changes of bacterial 16S rRNA gene abundance, and were significantly lower in August than in the other months for all three forest types (Supplementary Fig. 1).

The symbiotrophic fungi (Supplementary Fig. 2; 2.0%–81.1% of total fungi) tended to have a higher relative abundance throughout all sampling months and forest types than the saprotrophic fungi (Supplementary Fig. 2; 0.3%–30.5% of total fungi), and most of the symbiotrophic fungi belonged to the ectomycorrhizal guilds (Supplementary Fig. 3; 61.2%–100% of symbiotrophic fungi). The relative abundance of the ectomycorrhizal fungi differed significantly among sampling months (two-way ANOVA: $F = 13.65$ and $p < 0.001$), and the abundance was significantly higher in August than in the other sampling months (Fig. 4). The relative abundance of the saprotrophic fungi also differed significantly among sampling months and forest types (two-way ANOVA: $F = 4.65$, $p < 0.05$ and $F = 3.88$, $p < 0.05$ for months and forest types, respectively), and the abundance was significantly lower in August (2.7% ± 1.6% of total fungi) than in November (9.1% ± 9.1% of total fungi) and in Fir (2.1% ± 1.2% of total fungi) than in Larch (10.8% ± 7.4% of total fungi). The estimated absolute abundances of symbiotrophic and ectomycorrhizal fungi differed among sampling months (Supplementary Fig. 4; two-way ANOVA: $F = 3.74$ and $p < 0.01$, and $F = 3.87$ and $p < 0.01$, respectively), reflecting the results of the relative abundance of trophic modes and

370 the guild (Supplementary Fig. 2 and 3) rather than the total abundance of fungi (Fig. 2c).

371 The relative abundances of bacterial functional genes had significant correlations with
372 chemical properties (Supplementary Table 3). In particular, the C/N ratio was positively and strongly
373 correlated with chitinase, NAGase, leucine aminopeptidase, and arginase, and negatively correlated
374 with urease (Supplementary Table 3; $R^2 = 0.37$ and $p < 0.001$, $R^2 = 0.32$ and $p < 0.001$, $R^2 = 0.48$ and
375 $p < 0.001$, $R^2 = 0.43$ and $p < 0.001$, and $R^2 = 0.25$ and $p < 0.001$, respectively). Only weak
376 correlations were found between fungal groups of higher relative abundances (symbiotrophic,
377 saprotrophic, and ectomycorrhizal fungi) and chemical properties, such as pH and the C/N ratio
378 (Supplementary Table 3). The relative abundance of saprotrophic fungi positively correlated with
379 moisture content (Supplementary Table 3; $R^2 = 0.09$ and $p < 0.05$) and the relative abundance of
380 ectomycorrhiza negatively correlated with pH (Supplementary Table 3; $R^2 = 0.16$ and $p < 0.01$). The
381 relative abundances of chitinase, NAGase, leucine aminopeptidase, and arginase were significantly
382 and negatively correlated with net nitrification potential (Supplementary Table 3; $R^2 = 0.16$ and $p <$
383 0.01, $R^2 = 0.29$ and $p < 0.001$, $R^2 = 0.17$ and $p < 0.01$, and $R^2 = 0.14$ and $p < 0.01$, respectively), and
384 urease had a significant and positive relationship with net nitrification (Supplementary Table 3; $R^2 =$
385 0.27 and $p < 0.001$). The net mineralisation potential had a significant negative relationship with
386 NAGase only (Supplementary Table 3; $R^2 = 0.08$ and $p < 0.05$). The relative abundances of the
387 fungal groups did not have significant relationships with N mineralisation potentials (Supplementary
388 Table 3).

389 The relationships between the estimated absolute abundances of the bacterial functional
390 genes and fungi groups, and the net N mineralisation potentials are shown in Supplementary Fig. 5.
391 The bacterial functional genes, except urease, were significantly and negatively correlated with net
392 nitrification potentials (Supplementary Fig. 5; $R^2 = 0.10$ and $p < 0.05$ for chitinase, $R^2 = 0.09$ and $p <$
393 0.05 for NAGase, $R^2 = 0.07$ and $p < 0.05$ for leucine aminopeptidase, and $R^2 = 0.08$ and $p < 0.05$).

394 The estimated absolute abundances of the fungal groups had no significant correlations with net N
395 transformation processes (Supplementary Fig. 5).
396
397 *Modules and microbial functions in the co-occurrence network and their relationships with net N*
398 *transformation potentials*
399
400 The microbial co-occurrence network was divided into 13 modules (Fig. 5a). Modules 1 to 6 had a
401 higher number of OTUs belonging to the modules (12–18 OTUs) and higher relative abundances
402 representing these larger modules, while modules 7 to 13 had only 2 to 4 OTUs and lower relative
403 abundances, except for module 9, which occupied 9.76% of the total fungal community (Fig. 5b, c);
404 further analyses focused on modules 1 to 6. The relatively higher numbers of OTUs within modules
405 2 to 4 belonged to the phylum Acidobacteria (Fig. 5b; 10, 5, and 14 OTUs for each module,
406 respectively), and most of the Acidobacteria belonged to order Acidobacteriales (class
407 Acidobacteria) in module 3, while there were many OTUs belonging to Ellin6513 (class DA052) in
408 modules 2 and 4 (Supplementary Fig. 6 and Supplementary Table 4). Modules 5 and 6 had 8 and 10
409 OTUs belonging to the phylum Proteobacteria, respectively (Fig. 5b). Module 1 tended to have
410 many OTUs of the Proteobacteria and Bacteroidetes (Fig. 5b and Supplementary Fig. 4).
411 The OTUs that were predicted to have the genes responsible for N degradation enzymes
412 (chitinase, NAGase, leucine aminopeptidase, arginase, and urease) and for nitrification enzymes
413 (ammonia oxidation, hydroxylamine oxidation, and nitrite oxidation) investigated in this study were
414 depicted in the co-occurrence network, as shown in Figs. 6 and 7, respectively. Most of the OTUs in
415 the microbial co-occurrence network were predicted to have genes encoding NAGase and leucine
416 aminopeptidase regardless of the modules, while the numbers of OTUs having other functional
417 genes differed among modules (Fig. 6). The OTUs belonging to modules 2, 3, and 4 tended to have

418 the gene encoding chitinase, while relatively lower rates of the OTUs belonging to modules 5 and 6
419 were predicted to have that gene (Fig. 6a). In contrast, many OTUs belonging to modules 5 and 6
420 were predicted to have the gene responsible for urease, while modules 2, 3, and 4 had no or very few
421 OTUs predicted to have the gene (Fig. 6d). There was no OTU that was predicted to have the genes
422 responsible for ammonia monooxygenase, which is involved in the step from ammonia to
423 hydroxylamine (K10944, K10945, and K10946) in the co-occurrence network (Fig. 7a). Some links
424 between the OTUs that were predicted to have the gene responsible for hydroxylamine oxidation
425 (K10535), and the OTUs that were predicted to have at least one gene responsible for nitrite
426 oxidation (K00370, K00371) could be detected in module 6 and partly in module 5 (Fig. 7b, c). The
427 genes for denitrification were also depicted in the co-occurrence network (Supplementary Fig. 7).
428 There was only one link in module 1 between the first two steps, while some links were found in
429 modules 4, 5, and 6 for nitric oxide production and consumption, and in modules 2 and 4 for the
430 nitrous oxide production and consumption (Supplementary Fig. 7).
431 The sampling month did not significantly affect the relative abundances of modules 1 to 6
432 (Supplementary Fig. 8). The relative abundances of modules 1 to 3 and 6 had significant positive or
433 negative correlations with forest types; for example, module 1 had a significantly higher relative
434 abundance in the natural forest, while it was significantly lower in the fir forest (Supplementary Fig.
435 8; $R^2 = 0.32$ and $p < 0.001$, and $R^2 = 0.20$ and $p < 0.001$, respectively). There was no significant
436 relationship between modules 4 and 5, and forest types (Supplementary Fig. 8). The net nitrification
437 potential had significant positive correlations with the relative abundances of modules 1 and 5, and
438 negative correlations with modules 2 and 4 (Fig. 8a; $R^2 = 0.40$ and $p < 0.001$, $R^2 = 0.10$ and $p < 0.05$,
439 $R^2 = 0.07$ and $p < 0.05$, and $R^2 = 0.18$ and $p < 0.001$, respectively). On the contrary, the net
440 mineralisation potential only had a significant positive correlation with module 1 (Fig. 8a; $R^2 = 0.16$
441 and $p < 0.01$). The chemical properties were also significantly and positively or negatively correlated

with individual modules, particularly pH, moisture content and the C/N ratio were significantly correlated with the relative abundances of the modules (Supplementary Fig. 9).

The estimated absolute abundances of modules 1 to 6, calculated by multiplying the total bacterial 16S rRNA and fungal ITS genes, were significantly and negatively correlated with the month of August (Supplementary Fig. 10; from module 1 to 6, $R^2 = 0.17$ and $p < 0.01$, $R^2 = 0.16$ and $p < 0.01$, $R^2 = 13$ and $p < 0.01$, $R^2 = 0.16$ and $p < 0.01$, $R^2 = 0.10$ and $p < 0.05$, and $R^2 = 0.18$ and $p < 0.001$, respectively), which reflected the temporal changes of the total bacterial 16S rRNA gene abundance (Fig. 2a). There were no significant correlations between the estimated absolute abundances of the modules and the other sampling months (Supplementary Fig. 10). The effects of forest types on the estimated absolute abundances of modules 1 to 6 showed similar trends with the relative abundances, e.g. the estimated absolute abundance of module 1 was higher in the natural forest and lower in the fir forest (Supplementary Fig. 10; $R^2 = 0.15$ and $p < 0.01$, and $R^2 = 0.16$ and $p < 0.01$, respectively). The net nitrification potential had a significant positive correlation with the estimated absolute abundance of module 1 and a negative correlation with module 4 (Fig. 8b; $R^2 = 0.20$ and $p < 0.001$, and $R^2 = 0.16$ and $p < 0.01$, respectively). There was no significant relationship between the estimated absolute abundances of modules 1 to 6 and the net mineralisation potential (Fig. 8b).

Discussion

Differences in microbial communities and N transformation among seasons and forest types

We hypothesised that microbial abundance and functional communities changed due to the differences in seasons and/or forest types (hypothesis 1). Regarding this hypothesis, the effect of season on microbial abundance and functional communities was more significant than the effect of forest type (Figs. 2 and 4). However, the effect of season differed between bacteria and fungi, i.e. seasonal differences were apparent for the total abundance of bacteria and for the functional compositions of the fungi (Figs. 2 and 4). In the mid-summer, trees allocate more of their newly synthesised carbon to ectomycorrhizal fungi (EMF) (Högberg *et al.*, 2010) in order to take up more nutrients (Gessler *et al.*, 1998). The seasonal differences of carbon allocation from trees to EMF would explain the higher relative abundance of ectomycorrhizal guilds in mid-summer. In contrast, the abundance of saprotrophic fungi was suppressed in the mid-summer. Saprotrophic fungi decrease in abundance with increasing aridity (Tatsumi *et al.,* 2019). This suggests that the lower soil moisture content in the mid-summer (Supplementary Table 1) could lead to the lower relative abundance of saprotrophic fungi. Another explanation of a lower relative abundance of saprotrophic fungi was the suppression by the EMF. Ectomycorrhizal fungi have been reported to compete for resources with saprotrophic fungi (Lindahl *et al.*, 2002; Bödeker *et al.*, 2016). EMF are also strong competitors for nutrients with free-living microbes, including bacteria (Averill *et al.*, 2014; Tatsumi *et al.*, 2020). Furthermore, EMF have the ability to produce antibacterial material that could suppress bacterial species (Assigbetse *et al.*, 2005; Brooks *et al.*, 2011; Shirakawa *et al.*, 2019). Thus, the total bacterial abundance was probably suppressed in mid-summer due to the increase in EMF (Fig. 2). Another possible explanation for the seasonality of bacterial abundances was the seasonal changes in

484 environmental conditions. Among the chemical properties, only the pH significantly and positively
485 affected bacterial gene abundance (Supplementary Table 2). This was consistent with previous
486 findings (Rousk *et al.*, 2009, 2010). Thus, the lower pH in the mid-summer also might affect the
487 bacterial abundance. Osburn et al. (2018) found that similar seasonal trends of bacterial and fungal
488 abundances and reported that soil drying in summer decreased the bacterial abundance, while fungal
489 abundance was maintained potentially by the stimulation of mycorrhizal growth by carbon supply
490 from tree roots. In the present study, we could not find such interactions based on the correlational
491 analysis using all data; however, there was still the possibility that the soil moisture content
492 regulated the balance of soil microbial abundance. Although the environmental preferences differ
493 among bacterial species (Supplementary Fig. 9), the soil environmental condition might strongly
494 affect the total bacterial abundance and functional gene abundances.

495 The abundances of the fungal functional groups, particularly the saprotrophic fungi, varied
496 among forest types (Supplementary Fig. 2). The saprotrophic fungi are the main decomposers of
497 recalcitrant organic matter and obtain their energy and carbon sources from litter decomposition
498 (Osono, 2007; Uroz *et al.*, 2016). In general, the evergreen litter (Fir) decomposed slower than the
499 deciduous litters (Larch and Natural), partly because of the accumulation of recalcitrant organic
500 matter in the fir litter (Cornwell *et al.*, 2008). This difference of decomposability would affect the
501 energy acquisition of the saprotrophic fungi. Therefore, the EMF would be still active in the fir
502 forest due to the carbon supply from symbiotic trees, while the saprotrophic fungi might be
503 suppressed by the substrate recalcitrance.

504 Significant differences in the bacterial community structures among seasons and forest
505 types were observed (Nakayama *et al.,* 2019). Surprisingly, the relative abundances of the bacterial
506 functional genes concerning the N mineralisation process were stable across seasons and forest types
507 (Fig. 3). One explanation for this is the functional redundancy of the bacterial community

(Nannipieri *et al.*, 2003; Wertz *et al.*, 2006). Frossard *et al*. (2012) reported that there were no relationships between bacterial community structures and potential enzymatic activities because of bacterial functional redundancy. Thus, even if the microbial community structures changed among forest types, the potential to produce extracellular enzymes by the microbes would be maintained in these sites. Another explanation is the methodological limitations of PICRUSt, such as shortage of referenced reference database and restricted OTUs generation method (Douglas et al., 2020). Although PICRUSt has been widely used in the study of soil bacterial functional community (e.g., Isobe et al., 2018), other methods such as shotgun metagenomic sequencing should be considered for more detailed functional community analysis.

The N mineralisation potentials had no consistent relationships with total microbial abundances and functional groups among seasons as well as forest types. Thus, our second hypothesis that the differences in microbial abundance and functional communities regulated the changes of N transformation did not hold. In contrast to the microbial communities not varying among forest types, N mineralisation potentials varied among forest types (Fig. 1). There were three possible explanations for this result. First, litter quality may exert a stronger control on N mineralisation than the microbial factors. Based on the mycorrhizal associated nutrient economy theory (Phillips et al., 2013), the EMF-dominated forest stands, such as the plots in this study tend to have “organic nutrient economy” characterized by slow litter decomposition, and the organic N turnover regulates N availability in the soil (Phillips et al., 2013). As we discussed above, deciduous tree has higher decomposition rate than evergreen. In general, conifer leaves (Larch and Fir) also tend to have a slower decomposition rate than broad leaves (Natural) (Singh and Gupta, 1977). Accordingly, the N transformations might be faster in Natural than Larch and Fir, regardless of microbial dynamics. Second, we measured net N mineralisation and the functional attributes we characterized are more specifically focused on N acquiring enzymes. However, microbial

communities also consume mineralised N. While microbial N consumption was not measured and not known in this study, Urakawa *et al.* (2016) reported that the net rates of N mineralisation correlated with its gross rates, respectively, by investigating the net and gross rates of the N transformation processes in 38 forest sites across the Japan archipelago including the sites of this study. Further, some previous studies have reported significant relationships between microbial properties and the net N mineralisation rate (Fraterrigo *et al.,* 2006; Kang *et al.,* 2018). However, there is still the possibility that microbial N consumption masks the relationships between microbes and N transformations, and future research using the gross measurement of N mineralisation is needed to test this. The third possible explanation was that a part of microbial dynamics was important for N mineralisation potentials rather than whole microbial and functional gene abundance. Most bacterial species are considered to relate to N mineralisation (Bottomley et al., 2012; Isobe and Ohte, 2014). Furthermore, strong correlations between enzymatic activities and microbial functional predictions have been reported (Trivedi *et al.*, 2016). However, microbial activity varies widely among species (Fierer *et al.*, 2007; Pinnell *et al.*, 2014; Wilhelm *et al.*, 2019). Thus, as we discuss below for our third and fourth hypotheses, there is the possibility that a subsection of the microbial communities is more active and important for N mineralisation.

In terms of the nitrification process, positive relationships between ammonia-oxidising communities and nitrification have been previously reported (Hawkes *et al.*, 2005; Jia and Conrad, 2009; Isobe *et al.*, 2015). However, we could not find any significant relationships between them (Supplementary Table 2). Although the ammonia-oxidising prokaryotes markedly increased in mid-summer, the nitrification potential was stable across the seasons. The activities of the ammonia-oxidising prokaryotes are sensitive to environmental conditions, including pH and temperature (Jung *et al.*, 2011; Yao *et al.*, 2011; Zhang *et al.*, 2012; Taylor *et al.*, 2017). The activities of nitrifying communities might be low in the mid-summer in our study site because of the

lower pH, although further research focusing on the gross nitrification is needed as we discussed above. Furthermore, the proportions of the net nitrification and mineralisation potentials suggest that most of the mineralised N underwent the steps of nitrification at this study site (Fig. 1). The mineralisation step might limit the nitrification potentials at the site. There was also another explanation. In this study, we measured bacterial and archaeal *amoA* genes as the microbial factors because the *amoA* genes involved in the ammonia-oxidation, the first and rate-limiting step of nitrification (Isobe et al., 2011). Indeed, Isobe et al. (2018) reported that gross nitrification rete and soil NO_3^- concentration related to the AOB population in the natural forest of this study site. However, some bacteria completely oxidize ammonium into nitrate, which is called comammox, and has different enzymes from AOB (Costa et al., 2006). Comammox could be the main driver of nitrification in some ecosystems (Osburn and Barrett, 2020). A part of fungal groups also involved in the nitrification processes (Zhu et al., 2015). Thus, those other nitrifying communities that we did not measure might drive the nitrification process.

Modules in the microbial co-occurrence network

Our results showed that each module was differently related to N transformation processes at the site. Namely, modules 1 and 5 had significant positive relationships with N transformation processes and modules 2 and 4 had significant negative relationships (Fig. 8). These results affirmed our third hypothesis that individual modules in the co-occurrence network each had relationships with N mineralisation and nitrification potentials.

Bacterial species belonging to the Proteobacteria and Bacteroidetes, the main members of modules 1 and 5 (Fig. 5b), tend to have higher abundances in nutrient rich conditions (Fierer *et al.*, 2012; Peiffer *et al.*, 2013), implying their copiotrophic strategy. Copiotrophs are reported to have

high population turnover and short mean generation time (Fierer *et al.*, 2007). The microbial necromass is a significant source of dissolved organic matter and is recycled and mineralised by microbes (Miltner *et al.*, 2012; Huygens *et al.*, 2016). Hence, *r*-selected bacterial species could lead to more active mineralisation. However, module 6, which consisted mainly of Proteobacteria, did not correlate with net mineralisation potentials (Figs. 5 and 8). The phylum Proteobacteria is the largest bacterial phylum and contains diverse OTUs with diverse functions and metabolisms; even within the same class, their metabolisms vary (Kersters *et al.*, 2006). Therefore, our results indicate that modules 1 and 5 might include OTUs responsible for creating the variation of mineralisation potential, while there might be less important Proteobacteria within module 6. Future research highlighting the members within modules 1 and 5 can reveal the detailed relationships between microbial subgroups and the N transformation processes.

In contrast, modules 2 and 4, consisting mainly of the OTUs from the order Ellin6513 (Acidobacterial subdivision 2), significantly and negatively correlated with the net mineralisation potentials (Fig. 6 and Supplementary Table 4). The abundance of module 2 differed among forest types, while there were no clear trends for module 4 (Supplementary Figs. 8 and 10). Some of the members of the Acidobacteria adapt to oligotrophic conditions, having the *K*-selected strategy (Fierer *et al.*, 2007; Kielak *et al.*, 2016). Oligotrophic and *K*-selected bacteria have low growth rates, slow population turnover rates and long generation times (Fierer *et al.*, 2007). Therefore, modules 2 and 4 might have lower mineralisation potentials than the other modules. Further, modules 2 and 4 tended to have higher relative abundances within lower pH conditions (Supplementary Fig. 9). Previous studies have reported that the relative abundance of Acidobacteria, including subdivision 2, was negatively correlated with pH, while other bacterial phyla tended to correlate positively with pH (Lauber *et al.*, 2009; Rousk *et al.*, 2010). In the lower pH environments that the microbes from modules 2 and 4 were abundant in, other bacteria, including the Proteobacteria, would have been

suppressed.

The possibility that the litter quality rather than microbial community determined the N transformation processes discussed above still could not be rejected. However, the microbial subgroups would be important for the net N transformation processes at the site. We expected that the modules that fluctuated with differences in seasons and forest types were particularly important for the N mineralisation and nitrification potentials in our fourth hypothesis. Indeed, module 1, which had the strongest positive correlations with net N mineralisation and nitrification, varied among the forest types (Supplementary Fig. 8). However, module 5, which also had significant and positive relationships with net nitrification, did not vary among forest types (Supplementary Fig. 8).

Further, the relative abundances of analysed microbial modules did not fluctuate seasonally. This was consistent with bacterial community structures and functions (Fig. 3). These results of seasonally stable relative abundances of modules imply that at least core microbial species, which would be important for N transformations, had similar seasonal trends of growth and death. Therefore, our fourth hypothesis was partly affirmed but largely did not hold.

The co-occurrence network was constructed mathematically based only on the relative abundance data (Deng *et al.*, 2012). Therefore, it was difficult to separate whether the co-occurring links between two microbial species were actual interactions, such as substrate giving-receiving, or environmental filtering (e.g. niche preferences). In this study, there were only a few links of predicted enzymatic production within the modules in the co-occurrence network (Fig. 7 and Supplementary Fig. 7). Furthermore, individual modules had individual correlations with environmental factors (Supplementary Fig. 9), as shown in previous studies (Deng *et al.*, 2012; de Menezes *et al.*, 2015; Purahong *et al.*, 2016). Thus, the modules of the microbial co-occurrence networks may represent the niche separations of the microbial communities rather than interactions and physical links. Therefore, our results indicate that the niches of microbial sub-communities are

628 the factors important for N mineralisation processes.

629

630 *Conclusions*

631

632 In this study, the results showed that the abundances of microbial communities differed among
633 seasons. However, these seasonal fluctuations of microbial abundances were not related to the net N
634 mineralisation potentials. Instead, the importance of microbial modular sub-groups that shared
635 similar niches for the net N transformation potentials was revealed by the analysis of the
636 co-occurrence network and functional predictions. In this study, because low sequencing reads were
637 obtained and prevented us from analysing rare microbial communities, we focused on the core soil
638 microbial community in the network analysis. Since the network analysis is based on the correlation
639 of (relative) abundance, the difference in total sequence read numbers is not a major problem.
640 Therefore, in future research, the combination of 16S rRNA, amoA, and other functional genes with
641 the network analysis also could be adapted to analyse rare microbes with the core microbial
642 communities as used in this study for bacterial-fungal relationships. Although further research
643 investigating the detailed ecology and functions of the detected microbial subgroups is needed, our
644 findings and approaches provide a key for revealing N cycling by microbial communities in forest
645 soil.

646

References

Aber, J.D., Melillo, J.M., Nadelhoffer, K.J., McClaugherty, C.A., and Pastor, J. (1985) Fine root turnover in forest ecosystems in relation to quantity and form of nitrogen availability: a comparison of two methods. *Oecologia* **66**: 317–321.

Amann, R.I., Binder, B.J., Olson, R.J., Chisholm, S.W., Devereux, R., and Stahl, D.A. (1990) Combination of 16S rRNA-targeted oligonucleotide probes with flow cytometry for analyzing mixed microbial populations. *Appl Environ Microbiol* **56**: 1919–25.

Assigbetse, K., Gueye, M., Thioulouse, J., and Duponnois, R. (2005) Soil Bacterial Diversity Responses to Root Colonization by an Ectomycorrhizal Fungus are not Root-Growth-Dependent. *Microb Ecol* **50**: 350–359.

Averill, C., Turner, B.L., and Finzi, A.C. (2014) Mycorrhiza-mediated competition between plants and decomposers drives soil carbon storage. *Nature* **505**: 543–545.

Barberán, A., Bates, S.T., Casamayor, E.O., and Fierer, N. (2012) Using network analysis to explore co-occurrence patterns in soil microbial communities. *ISME J* **6**: 343–351.

Bastian, M., Heymann, S., and Jacomy, M. (2009) Gephi: An Open Source Software for Exploring and Manipulating Networks. In, *Proceedings of the Third International ICWSM Conference*., pp. 361–362.

Bödeker, I.T.M., Lindahl, B.D., Olson, Å., and Clemmensen, K.E. (2016) Mycorrhizal and saprotrophic fungal guilds compete for the same organic substrates but affect decomposition differently. *Funct Ecol* **30**: 1967–1978.

Bottomley, P.J., Taylor, A.E., and Myrold, D.D. (2012) A consideration of the relative contributions of different microbial subpopulations to the soil N cycle. *Front Microbiol* **3**: 373.

Boyle, S.A., Yarwood, R.R., Bottomley, P.J., and Myrold, D.D. (2008) Bacterial and fungal contributions to soil nitrogen cycling under Douglas fir and red alder at two sites in Oregon. *Soil Biol Biochem* **40**: 443–451.

Brooks, D.D., Chan, R., Starks, E.R., Grayston, S.J., and Jones, M.D. (2011) Ectomycorrhizal hyphae structure components of the soil bacterial community for decreased phosphatase production. *FEMS Microbiol Ecol* **76**: 245–255.

Caffrey, J.M., Bano, N., Kalanetra, K., and Hollibaugh, J.T. (2007) Ammonia oxidation and ammonia-oxidizing bacteria and archaea from estuaries with differing histories of hypoxia. *ISME J* **1**: 660–662.

Chao, Y., Liu, W., Chen, Y., Chen, W., Zhao, L., Ding, Q., et al. (2016) Structure, Variation, and Co-occurrence of Soil Microbial Communities in Abandoned Sites of a Rare Earth Elements Mine. *Environ Sci Technol* **50**: 11481–11490.

682 Clauset, A., Newman, M.E.J., and Moore, C. (2004) Finding community structure in very large networks.
683 *Phys Rev* **70**: 066111.
684 Cornwell, W.K., Cornelissen, J.H.C., Amatangelo, K., Dorrepaal, E., Eviner, V.T., Godoy, O., et al.
685 (2008) Plant species traits are the predominant control on litter decomposition rates within biomes
686 worldwide. *Ecol Lett* **11**: 1065–1071.
687 Costa, E., Pérez, J., and Kreft, J.U. (2006) Why is metabolic labour divided in nitrification? *Trends*
688 *Microbiol* **14**: 213–219.
689 Deng, Y., Jiang, Y.H., Yang, Y., He, Z., Luo, F., and Zhou, J. (2012) Molecular ecological network
690 analyses. *BMC Bioinformatics* **13**: 113.
691 Douglas, G.M., Maffei, V.J., Zaneveld, J.R., Yurgel, S.N., Brown, J.R., Taylor, C.M., et al. (2020)
692 PICRUSt2 for prediction of metagenome functions. *Nat Biotechnol* **38**: 685–688.
693 Ekblad, A., Wallander, H., Godbold, D.L., Cruz, C., Johnson, D., Baldrian, P., et al. (2013) The
694 production and turnover of extramatrical mycelium of ectomycorrhizal fungi in forest soils: role in
695 carbon cycling. *Plant Soil* **366**: 1–27.
696 Fierer, N., Bradford, M.A., and Jackson, R.B. (2007) Toward an ecological classification of soil bacteria.
697 *Ecology* **88**: 1354–1364.
698 Fierer, N., Jackson, J.A., Vilgalys, R., and Jackson, R.B. (2005) Assessment of soil microbial community
699 structure by use of taxon-specific quantitative PCR assays. *Appl Environ Microbiol* **71**: 4117–20.
700 Fierer, N., Lauber, C.L., Ramirez, K.S., Zaneveld, J., Bradford, M.A., and Knight, R. (2012) Comparative
701 metagenomic, phylogenetic and physiological analyses of soil microbial communities across
702 nitrogen gradients. *ISME J* **6**: 1007–1017.
703 Fraterrigo, J.M., Balser, T.C., and Turner, M.G. (2006) Microbial community variation and its
704 relationship with nitrogen mineralization in historically altered forests. *Ecology* **87**: 570–579.
705 Frossard, A., Gerull, L., Mutz, M., and Gessner, M.O. (2012) Disconnect of microbial structure and
706 function: Enzyme activities and bacterial communities in nascent stream corridors. *ISME J* **6**:
707 680–691.
708 Gessler, A., Schneider, S., Von Sengbusch, D., Weber, P., Hanemann, U., Huber, C., et al. (1998) Field
709 and laboratory experiments on net uptake of nitrate and ammonium the roots of spruce (Picea abies)
710 and beech (Fagus sylvatica) trees. *New Phytol* **138**: 275–285.
711 Großkopf, R., Janssen, P.H., and Liesack, W. (1998) Diversity and structure of the methanogenic
712 community in anoxic rice paddy soil microcosms as examined by cultivation and direct 16S rRNA
713 gene sequence retrieval. *Appl Environ Microbiol* **64**: 960–969.
714 Gubry-Rangin, C., Nicol, G.W., and Prosser, J.I. (2010) Archaea rather than bacteria control nitrification
715 in two agricultural acidic soils. *FEMS Microbiol Ecol* **74**: 566–574.
716 Hawkes, C. V., Wren, I.F., Herman, D.J., and Firestone, M.K. (2005) Plant invasion alters nitrogen
717 cycling by modifying the soil nitrifying community. *Ecol Lett* **8**: 976–985.

718 Högberg, M.N., Briones, M.J.I., Keel, S.G., Metcalfe, D.B., Campbell, C., Midwood, A.J., et al. (2010)
719 Quantification of effects of season and nitrogen supply on tree below-ground carbon transfer to
720 ectomycorrhizal fungi and other soil organisms in a boreal pine forest. *New Phytol* **187**: 485–493.
721 Högberg, M.N., Högberg, P., and Myrold, D.D. (2007) Is microbial community composition in boreal
722 forest soils determined by pH, C-to-N ratio, the trees, or all three? *Oecologia* **150**: 590–601.
723 Huygens, D., Díaz, S., Urcelay, C., and Boeckx, P. (2016) Microbial recycling of dissolved organic
724 matter confines plant nitrogen uptake to inorganic forms in a semi-arid ecosystem. *Soil Biol*
725 *Biochem* **101**: 142–151.
726 Isobe, K., Ise, Y., Kato, H., Oda, T., Vincenot, C.E., Koba, K., et al. (2020) Consequences of microbial
727 diversity in forest nitrogen cycling: diverse ammonifiers and specialized ammonia oxidizers. *ISME*
728 *J* **14**: 12–25.
729 Isobe, K., Koba, K., Otsuka, S., and Senoo, K. (2011) Nitrification and nitrifying microbial communities
730 in forest soils. J For Res 16: 351–362.
731 Isobe, K. and Ohte, N. (2014) Ecological perspectives on microbes involved in N-cycling. *Microbes*
732 *Environ* **29**: 4–16.
733 Isobe, K., Ohte, N., Oda, T., Murabayashi, S., Wei, W., Senoo, K., et al. (2015) Microbial regulation of
734 nitrogen dynamics along the hillslope of a natural forest. *Front Environ Sci* **2**: 63.
735 Isobe, K., Oka, H., Watanabe, T., Tateno, R., Urakawa, R., Liang, C., et al. (2018) High soil microbial
736 activity in the winter season enhances nitrogen cycling in a cool-temperate deciduous forest. *Soil*
737 *Biol Biochem* **124**: 90–100.
738 IUSS Working Group WRB (2015) International soil classification system for naming soils and creating
739 legends for soil maps. World Reference Base for Soil Resources 2014, update 2015.
740 Iwaoka, C., Imada, S., Taniguchi, T., Du, S., Yamanaka, N., and Tateno, R. (2018) The Impacts of Soil
741 Fertility and Salinity on Soil Nitrogen Dynamics Mediated by the Soil Microbial Community
742 Beneath the Halophytic Shrub Tamarisk. *Microb Ecol* **75**: 985–996.
743 Jia, Z. and Conrad, R. (2009) Bacteria rather than Archaea dominate microbial ammonia oxidation in an
744 agricultural soil. *Environ Microbiol* **11**: 1658–1671.
745 Jones, C.M. and Hallin, S. (2019) Geospatial variation in co-occurrence networks of nitrifying microbial
746 guilds. *Mol Ecol* **28**: 293–306.
747 Jung, J., Yeom, J., Kim, J., Han, J., Lim, H.S., Park, H., et al. (2011) Change in gene abundance in the
748 nitrogen biogeochemical cycle with temperature and nitrogen addition in Antarctic soils. *Res*
749 *Microbiol* **162**: 1018–1026.
750 Kaiser, C., Fuchslueger, L., Koranda, M., Gorfer, M., Stange, C.F., Kitzler, B., et al. (2011) Plants control
751 the seasonal dynamics of microbial N cycling in a beech forest soil by belowground C allocation.
752 *Ecology* **92**: 1036–1051.
753 Kaiser, C., Koranda, M., Kitzler, B., Fuchslueger, L., Schnecker, J., Schweiger, P., et al. (2010)

754 Belowground carbon allocation by trees drives seasonal patterns of extracellular enzyme activities
755 by altering microbial community composition in a beech forest soil. *New Phytol* **187**: 843–858.
756 Kang, H., Gao, H., Yu, W., Yi, Y., Wang, Y., and Ning, M. (2018) Changes in soil microbial community
757 structure and function after afforestation depend on species and age: Case study in a subtropical
758 alluvial island. *Sci Total Environ* **625**: 1423–1432.
759 Kanehisa, M., Sato, Y., Kawashima, M., Furumichi, M., and Tanabe, M. (2016) KEGG as a reference
760 resource for gene and protein annotation. *Nucleic Acids Res* **44**: D457–D462.
761 Kersters, K., DeVos, P., Gills, M., Swings, J., Vandamme, P., and Stackebrandt, E. (2006) Introduction to
762 the proteobacteria. In, Dworkin,M., Falkow,S., Eosenberg,E., Schleifer,K.-H., and Stackbrandt,E.
763 (eds), *The prokaryotes*. New yo: Springer-Verlag, pp. 3–37.
764 Kielak, A.M., Barreto, C.C., Kowalchuk, G.A., van Veen, J.A., and Kuramae, E.E. (2016) The ecology of
765 Acidobacteria: Moving beyond genes and genomes. *Front Microbiol* **7**: 744.
766 Langfelder, P. and Horvath, S. (2007) Eigengene networks for studying the relationships between
767 co-expression modules. *BMC Syst Biol* **1**: 54.
768 Langfelder, P. and Horvath, S. (2008) WGCNA: an R package for weighted correlation network analysis.
769 *BMC Bioinformatics* **9**: 559.
770 Langille, M.G.I., Zaneveld, J., Caporaso, J.G., McDonald, D., Knights, D., Reyes, J.A., et al. (2013)
771 Predictive functional profiling of microbial communities using 16S rRNA marker gene sequences.
772 *Nat Biotechnol* **31**: 814–821.
773 Lauber, C.L., Hamady, M., Knight, R., and Fierer, N. (2009) Pyrosequencing-based assessment of soil pH
774 as a predictor of soil bacterial community structure at the continental scale. *Appl Environ Microbiol*
775 **75**: 5111–20.
776 Lauber, C.L., Strickland, M.S., Bradford, M.A., and Fierer, N. (2008) The influence of soil properties on
777 the structure of bacterial and fungal communities across land-use types. *Soil Biol Biochem* **40**:
778 2407–2415.
779 LeBauer, D.S. and Treseder, K.K. (2008) Nitrogen limitation of net primary productivity in terrestrial
780 ecosystems is globally distributed. *Ecology* **89**: 371–379.
781 Lindahl, B.O., Taylor, A.F.S., and Finlay, R.D. (2002) Defining nutritional constraints on carbon cycling
782 in boreal forests-towards a less “phytocentric” perspective. *Plant Soil* **242**: 123-135
783 Lladó, S., Žifčáková, L., Větrovský, T., Eichlerová, I., and Baldrian, P. (2016) Functional screening of
784 abundant bacteria from acidic forest soil indicates the metabolic potential of Acidobacteria
785 subdivision 1 for polysaccharide decomposition. *Biol Fertil Soils* **52**: 251–260.
786 Matsuoka, S., Sugiyama, Y., Tateno, R., Imamura, S., Kawaguchi, E., and Osono, T. (2020) Evaluation of
787 host effects on ectomycorrhizal fungal community compositions in a forested landscape in northern
788 Japan. *R Soc Open Sci* **7**: 191952.
789 Mendes, L.W., Kuramae, E.E., Navarrete, A.A., Van Veen, J.A., and Tsai, S.M. (2014) Taxonomical and

functional microbial community selection in soybean rhizosphere. *ISME J* **8**: 1577–1587.

de Menezes, A.B., Prendergast-Miller, M.T., Richardson, A.E., Toscas, P., Farrell, M., Macdonald, L.M., et al. (2015) Network analysis reveals that bacteria and fungi form modules that correlate independently with soil parameters. *Environ Microbiol* **17**: 2677–2689.

Miltner, A., Bombach, P., Schmidt-Brücken, B., and Kästner, M. (2012) SOM genesis: Microbial biomass as a significant source. *Biogeochemistry* **111**: 41–55.

Moore-Kucera, J. and Dick, R.P. (2008) PLFA profiling of microbial community structure and seasonal shifts in soils of a Douglas-fir chronosequence. *Microb Ecol* **55**: 500–511.

Muyzer, G., de Waal, E.C., and Uitterlinden, A.G. (1993) Profiling of complex microbial populations by denaturing gradient gel electrophoresis analysis of polymerase chain reaction-amplified genes coding for 16S rRNA. *Appl Environ Microbiol* **59**: 695–700.

Nakayama, M., Imamura, S., Taniguchi, T., and Tateno, R. (2019) Does conversion from natural forest to plantation affect fungal and bacterial biodiversity, community structure, and co-occurrence networks in the organic horizon and mineral soil? *For Ecol Manage* **446**: 238–250.

Nakayama, M. and Tateno, R. (2018) Solar radiation strongly influences the quantity of forest tree root exudates. *Trees* **32**: 871–879.

Nannipieri, P., Ascher, J., Ceccherini, M.T., Landi, L., Pietramellara, G., and Renella, G. (2003) Microbial diversity and soil functions. *Eur J Soil Sci* **54**: 655–670.

Newman, M.E.J. (2006) Modularity and community structure in networks. *Proc Natl Acad Sci U S A* **103**: 8577–8582.

Nguyen, N.H., Song, Z., Bates, S.T., Branco, S., Tedersoo, L., Menke, J., et al. (2016) FUNGuild: An open annotation tool for parsing fungal community datasets by ecological guild. *Fungal Ecol* **20**: 241–248.

Okano, Y., Hristova, K.R., Leutenegger, C.M., Jackson, L.E., Denison, R.F., Gebreyesus, B., et al. (2004) Application of Real-Time PCR To Study Effects of Ammonium on Population Size of Ammonia-Oxidizing Bacteria in Soil. *Appl Environ Microbiol* **70**: 1008–1016.

Osburn, E.D. and Barrett, J.E. (2020) Abundance and functional importance of complete ammonia-oxidizing bacteria (comammox) versus canonical nitrifiers in temperate forest soils. *Soil Biol Biochem* **145**: 107801.

Osburn, E.D., Elliottt, K.J., Knoepp, J.D., Miniat, C.F., and Barrett, J.E. (2018) Soil microbial response to Rhododendron understory removal in southern Appalachian forests: Effects on extracellular enzymes. *Soil Biol Biochem* **127**: 50–59.

Osono, T. (2007) Ecology of ligninolytic fungi associated with leaf litter decomposition. *Ecol Res* **22**: 955–974.

Peiffer, J.A., Spor, A., Koren, O., Jin, Z., Tringe, S.G., Dangl, J.L., et al. (2013) Diversity and heritability of the maize rhizosphere microbiome under field conditions. *Proc Natl Acad Sci U S A* **110**:

6548–6553.

Phillips, R.P., Brzostek, E., and Midgley, M.G. (2013) The mycorrhizal-associated nutrient economy: A new framework for predicting carbon-nutrient couplings in temperate forests. *New Phytol* **199**: 41–51.

Pinnell, L.J., Dunford, E., Ronan, P., Hausner, M., and Neufeld, J.D. (2014) Recovering glycoside hydrolase genes from active tundra cellulolytic bacteria. *Can J Microbiol* **60**: 469–476.

Prevost-Boure, N.C., Maron, P.A., Ranjard, L., Nowak, V., Dufrene, E., Damesin, C., et al. (2011) Seasonal dynamics of the bacterial community in forest soils under different quantities of leaf litter. *Appl Soil Ecol* **47**: 14–23.

Purahong, W., Krüger, D., Buscot, F., and Wubet, T. (2016) Correlations between the composition of modular fungal communities and litter decomposition-associated ecosystem functions. *Fungal Ecol* **22**: 106–114.

Raskin, L., Stromley, J.M., Rittmann, B.E., and Stahl, D.A. (1994) Group-specific 16S rRNA hybridization probes to describe natural communities of methanogens. *Appl Environ Microbiol* **60**: 1232–1240.

Reich, P.B., Grigal, D.F., Aber, J.D., and Gower, S.T. (1997) Nitrogen mineralization and productivity in 50 hardwood and conifer stands on diverse soils. *Ecology* **78**: 335–347.

Ribbons, R.R., Levy-Booth, D.J., Masse, J., Grayston, S.J., McDonald, M.A., Vesterdal, L., and Prescott, C.E. (2016) Linking microbial communities, functional genes and nitrogen-cycling processes in forest floors under four tree species. *Soil Biol Biochem* **103**: 181–191.

Rotthauwe, J.H., Witzel, K.P., and Liesack, W. (1997) The ammonia monooxygenase structural gene amoA as a functional marker: molecular fine-scale analysis of natural ammonia-oxidizing populations. *Appl Environ Microbiol* **63**: 4704–12.

Rousk, J., Bååth, E., Brookes, P.C., Lauber, C.L., Lozupone, C., Caporaso, J.G., et al. (2010) Soil bacterial and fungal communities across a pH gradient in an arable soil. *ISME J* **4**: 1340–1351.

Rousk, J., Brookes, P.C., and Bååth, E. (2009) Contrasting soil pH effects on fungal and bacterial growth suggest functional redundancy in carbon mineralization. *Appl Environ Microbiol* **75**: 1589–96.

Saiya-Cork, K.R., Sinsabaugh, R.L., and Zak, D.R. (2002) The effects of long term nitrogen deposition on extracellular enzyme activity in an Acer saccharum forest soil. *Soil Biol Biochem* **34**: 1309–1315.

Schimel, J.P. and Bennett, J. (2004) Nitrogen mineralization: Challenges of a changing paradigm. *Ecology* **85**: 591–602.

Shirakawa, M., Uehara, I., and Tanaka, M. (2019) Mycorrhizosphere Bacterial Communities and their Sensitivity to Antibacterial Activity of Ectomycorrhizal Fungi. *Microbes Environ* **34**: 191–198.

Singh, J.S. and Gupta, S.R. (1977) Plant decomposition and soil respiration in terrestrial ecosystems. *Bot Rev* **43**: 449–528.

Sinsabaugh, R.L., Lauber, C.L., Weintraub, M.N., Ahmed, B., Allison, S.D., Crenshaw, C., et al. (2008) Stoichiometry of soil enzyme activity at global scale. *Ecol Lett* **11**: 1252–1264.

Strickland, M.S., Lauber, C., Fierer, N., and Bradford, M.A. (2009) Testing the functional significance of microbial community composition. *Ecology* **90**: 441–451.

Sun, S., Li, S., Avera, B.N., Strahm, B.D., and Badgley, B.D. (2017) Soil bacterial and fungal communities show distinct recovery patterns during forest ecosystem restoration. *Appl Environ Microbiol* **83**: 966–983.

Tateno, R., Hishi, T., and Takeda, H. (2004) Above- and belowground biomass and net primary production in a cool-temperate deciduous forest in relation to topographical changes in soil nitrogen. *For Ecol Manage* **193**: 297–306.

Tatsumi, C., Taniguchi, T., Du, S., Yamanaka, N., and Tateno, R. (2020) Soil nitrogen cycling is determined by the competition between mycorrhiza and ammonia-oxidizing prokaryotes. *Ecology* **101**: e02963.

Tatsumi, C., Taniguchi, T., Du, S., Yamanaka, N., and Tateno, R. (2019) The steps in the soil nitrogen transformation process vary along an aridity gradient via changes in the microbial community. *Biogeochemistry* **144**: 15–29.

Taylor, A.E., Giguere, A.T., Zoebelein, C.M., Myrold, D.D., and Bottomley, P.J. (2017) Modeling of soil nitrification responses to temperature reveals thermodynamic differences between ammonia-oxidizing activity of archaea and bacteria. *ISME J* **11**: 896–908.

Toju, H., Kishida, O., Katayama, N., and Takagi, K. (2016) Networks depicting the fine-scale co-occurrences of fungi in soil horizons. *PLoS One* **11**: 1–18.

Toju, H., Tanabe, A.S., Yamamoto, S., and Sato, H. (2012) High-coverage ITS primers for the DNA-based identification of ascomycetes and basidiomycetes in environmental samples. *PLoS One* **7**: e40863.

Torsvik, V. and Øvreås, L. (2002) Microbial diversity and function in soil: from genes to ecosystems. *Curr Opin Microbiol* **5**: 240–245.

Tourna, M., Freitag, T.E., Nicol, G.W., and Prosser, J.I. (2008) Growth, activity and temperature responses of ammonia-oxidizing archaea and bacteria in soil microcosms. *Environ Microbiol* **10**: 1357–1364.

Trivedi, P., Delgado-Baquerizo, M., Trivedi, C., Hu, H., Anderson, I.C., Jeffries, T.C., et al. (2016) Microbial regulation of the soil carbon cycle: evidence from gene–enzyme relationships. *ISME J* **10**: 2593–2604.

Urakawa, R., Ohte, N., Shibata, H., Isobe, K., Tateno, R., Oda, T., et al. (2016) Factors contributing to soil nitrogen mineralization and nitrification rates of forest soils in the Japanese archipelago. *For Ecol Manage* **361**: 382–396.

Urbanová, M., Šnajdr, J., and Baldrian, P. (2015) Composition of fungal and bacterial communities in

forest litter and soil is largely determined by dominant trees. *Soil Biol Biochem* **84**: 53–64.

Uroz, S., Oger, P., Tisserand, E., Cébron, A., Turpault, M.-P., Buée, M., et al. (2016) Specific impacts of beech and Norway spruce on the structure and diversity of the rhizosphere and soil microbial communities. *Sci Rep* **6**: 27756.

Ushio, M., Kitayama, K., and Balser, T.C. (2010) Tree species-mediated spatial patchiness of the composition of microbial community and physicochemical properties in the topsoils of a tropical montane forest. *Soil Biol Biochem* **42**: 1588–1595.

Vitousek, P. and Howarth, R. (1991) Nitrogen limitation on land and in the sea: How can it occur? *Biogeochemistry* **13**: 87–115.

Wan, X., Huang, Z., He, Z., Yu, Z., Wang, M., Davis, M.R., and Yang, Y. (2015) Soil C:N ratio is the major determinant of soil microbial community structure in subtropical coniferous and broadleaf forest plantations. *Plant Soil* **387**: 103–116.

Wertz, S., Degrange, V., Prosser, J.I., Poly, F., Commeaux, C., Freitag, T., et al. (2006) Maintenance of soil functioning following erosion of microbial diversity. *Environ Microbiol* **8**: 2162–2169.

Wilhelm, R.C., Singh, R., Eltis, L.D., and Mohn, W.W. (2019) Bacterial contributions to delignification and lignocellulose degradation in forest soils with metagenomic and quantitative stable isotope probing. *ISME J* **13**: 413–429.

Yao, H., Gao, Y., Nicol, G.W., Campbell, C.D., Prosser, J.I., Zhang, L., et al. (2011) Links between ammonia oxidizer community structure, abundance, and nitrification potential in acidic soils. *Appl Environ Microbiol* **77**: 4618–25.

Zhang, L.-M., Hu, H.-W., Shen, J.-P., and He, J.-Z. (2012) Ammonia-oxidizing archaea have more important role than ammonia-oxidizing bacteria in ammonia oxidation of strongly acidic soils. *ISME J* **6**: 1032–1045.

Zhu, T., Meng, T., Zhang, J., Zhong, W., Müller, C., and Cai, Z. (2015) Fungi-dominant heterotrophic nitrification in a subtropical forest soil of China. *J Soils Sediments* **15**: 705–709.

925 Figure captions

926

927 **Fig. 1** Temporal changes of (a) the net nitrification and (b) the mineralisation potentials of Larch, Fir
928 and Natural forests. The values are means and bars represent the standard deviation. FT, M, and
929 F×M represent the results of the two-way ANOVA for forest types, sampling months, and the
930 interaction of forest type and sampling month, respectively. Symbols represent the following: n.s.
931 represents $p \geq 0.05$ and ** represents $p < 0.01$.

932

933 **Fig. 2** Gene abundances of (a) total bacteria, (b) total archaea, (c) total fungi, (d) AOB, and (e) and
934 AOA. The values are means and the bars represent standard deviations. FT, M, and F×M represent
935 the results of the two-way ANOVA for forest types, sampling months, and the interaction of forest
936 type and sampling month, respectively. Symbols represent the following: n.s. represents $p \geq 0.05$ and
937 *** represents $p < 0.001$.

938

939 **Fig. 3** Predicted counts of genes involved in nitrogen degradation and mineralisation from the
940 rarefied 1441 16S rRNA gene sequences. The values are means and the bars represent standard
941 deviations. FT, M, and F×M represent the results of two-way ANOVA for forest types, sampling
942 months, and the interaction of forest type and sampling month, respectively. Symbols represent the
943 following: n.s. represents $p \geq 0.05$ and * represents $p < 0.05$.

944

945 **Fig. 4** The predicted relative abundances of guilds within the symbiotrophic fungal group. The
946 values are means and the bars represent standard deviations. FT, M, and F×M represent the results of
947 the two-way ANOVA for forest types, sampling months, and the interaction of forest type and
948 sampling month, respectively. Symbols represent the following: n.s. represents $p \geq 0.05$ and ***

949 represents $p < 0.001$.

950

951 **Fig. 5** (a) The co-occurrence network divided by modules, (b) the taxa of the operational taxonomic
952 units (OTUs) belonging to each module, and (c) the average relative abundance of each module. The
953 average relative abundances of modules were calculated by summing the average relative
954 abundances of the OTUs belonging to each module.

955

956 **Fig. 6** The operational taxonomic units (OTUs) with the genes responsible for (a) chitinase, (b)
957 NAGase, (c) leucine aminopeptidase, (d) arginase, and (e) urease in the co-occurrence network.

958

959 **Fig. 7** The operational taxonomic units (OTUs) with the genes responsible for each nitrification step:
960 (a) ammonia to hydroxylamine, (b) hydroxylamine to nitrite, and (c) nitrite to nitrate in the
961 co-occurrence network.

962

963 **Fig. 8** The relationships between the nitrogen mineralisation potentials and (a) the relative
964 abundances and (b) the estimated absolute abundances of modules 1 to 6. Values in each cell
965 represent correlation coefficients by Pearson's correlation. Symbols represent the following: n.s., *,
966 **, and *** represent $p \geq 0.05$, $p < 0.05$, $p < 0.01$, and $p < 0.001$, respectively.

967

968

969

Fig. 1 Nakayama et al.

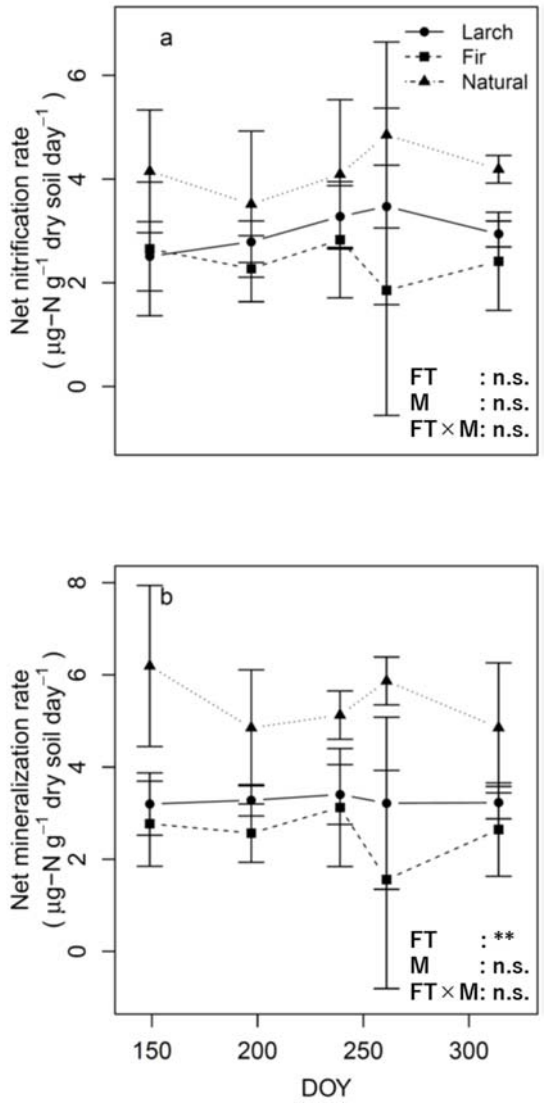

Fig. 2 Nakayama et al.

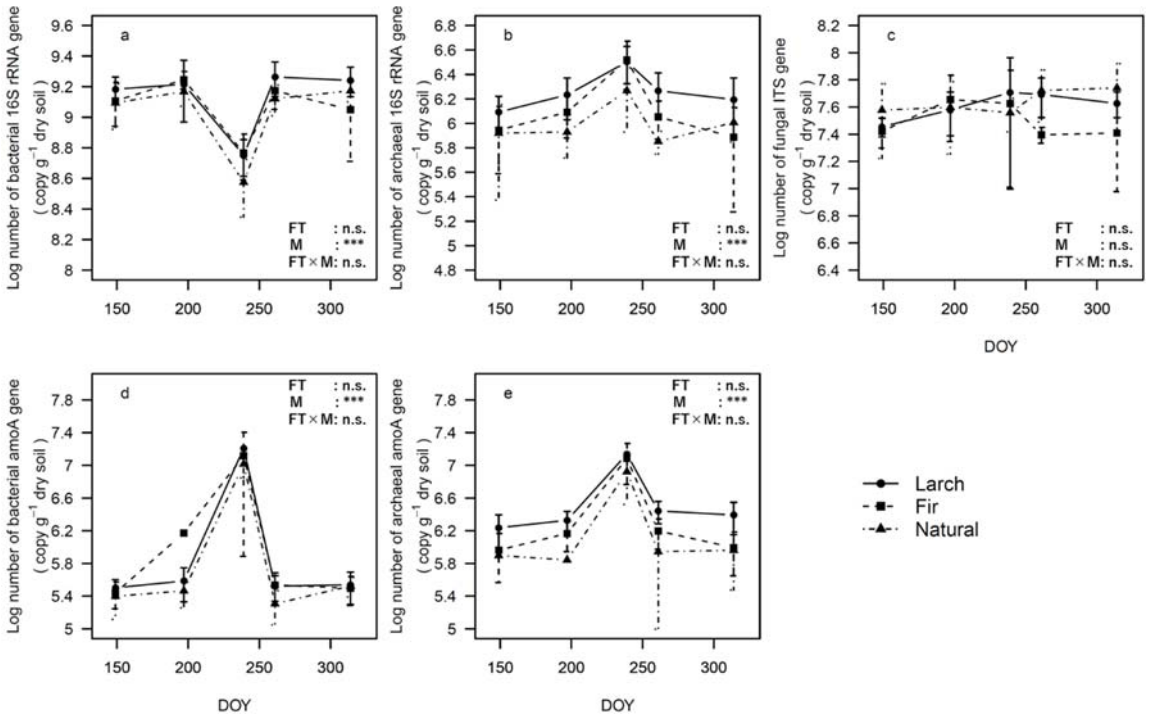

Fig. 3 Nakayama et al.

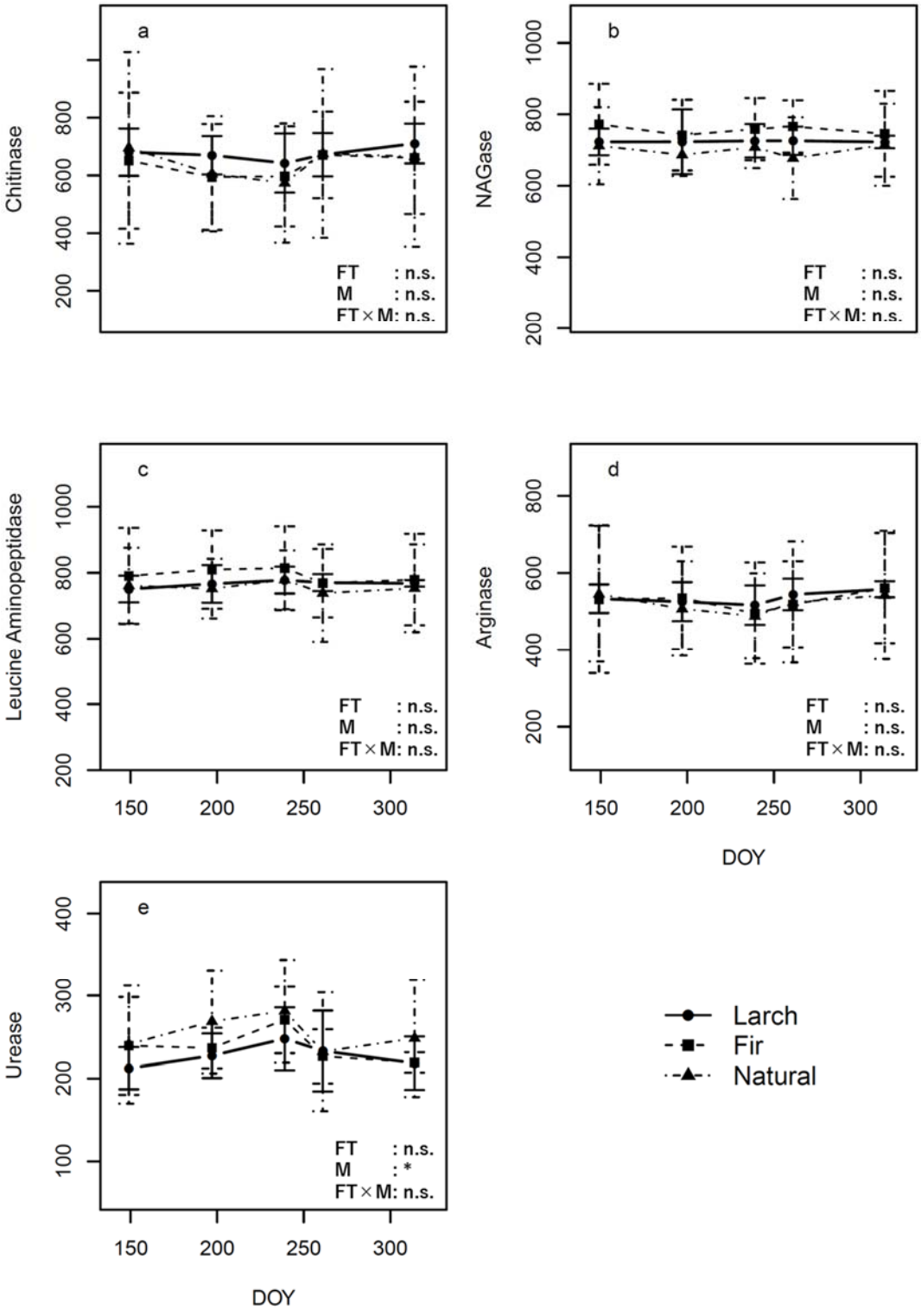

Fig. 4 Nakayama et al.

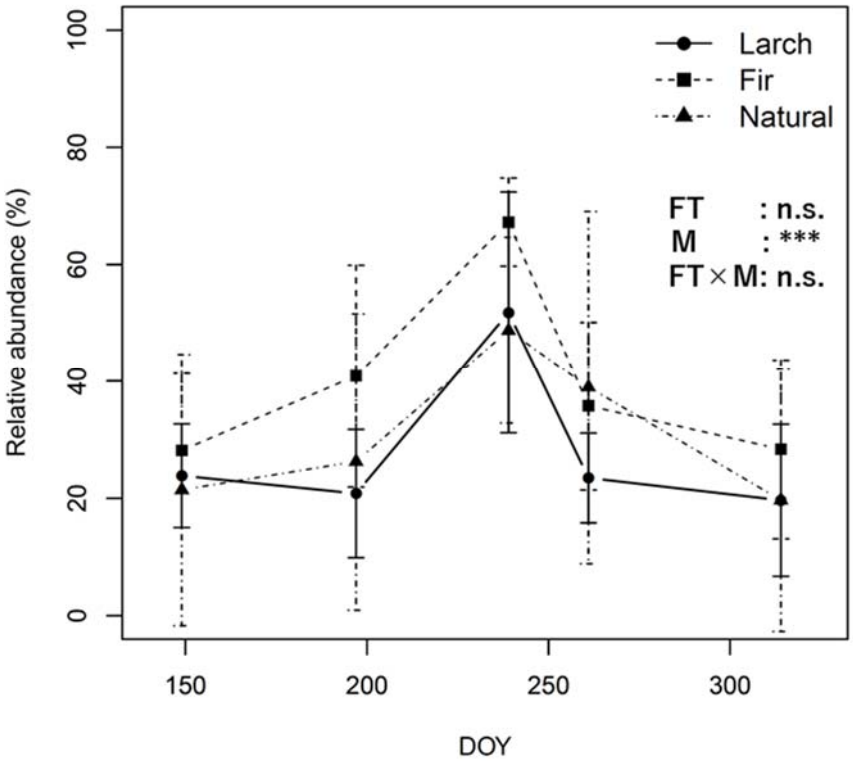

Fig. 5 Nakayama et al.

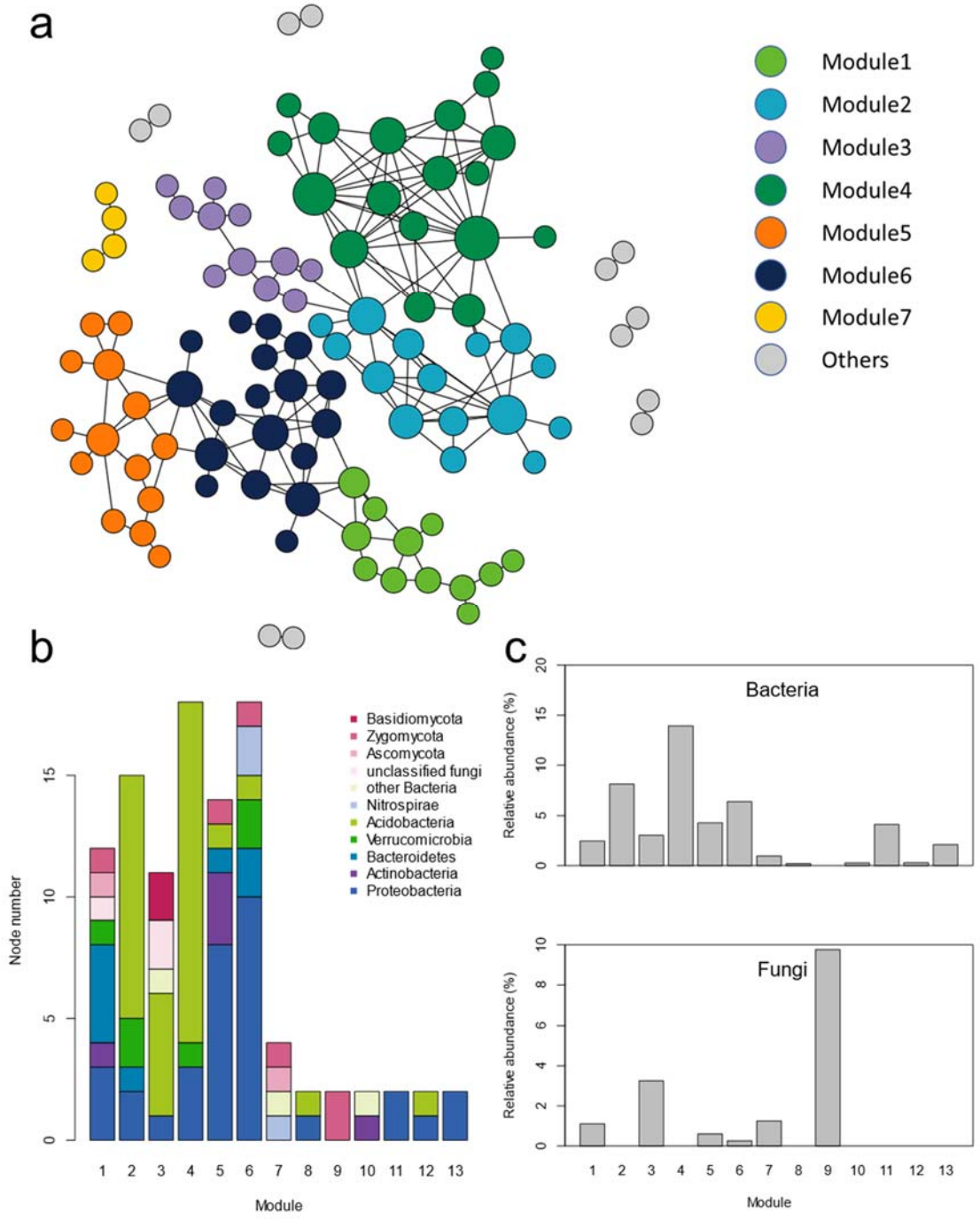

Fig. 6 Nakayama et al.

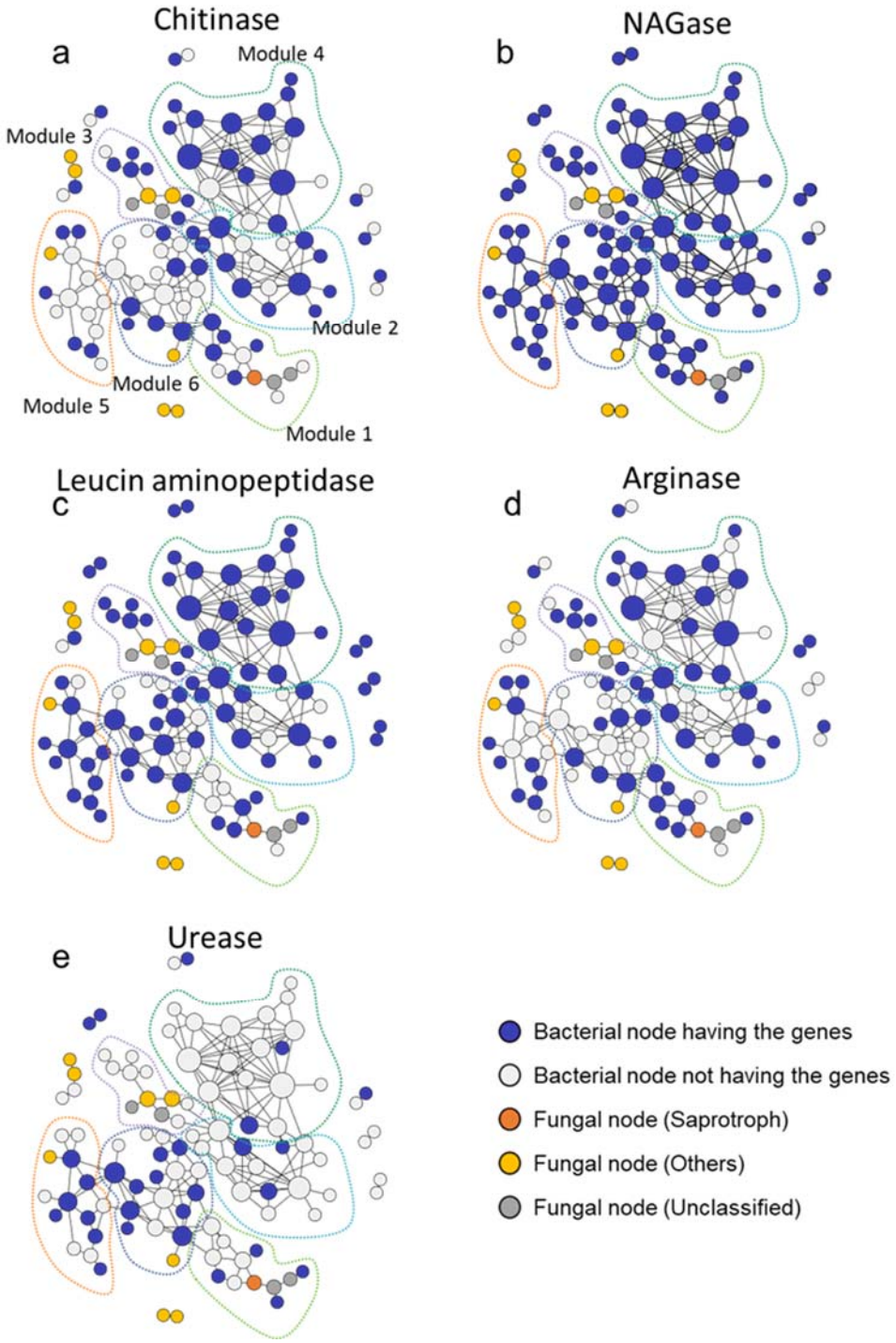

Fig. 7 Nakayama et al.

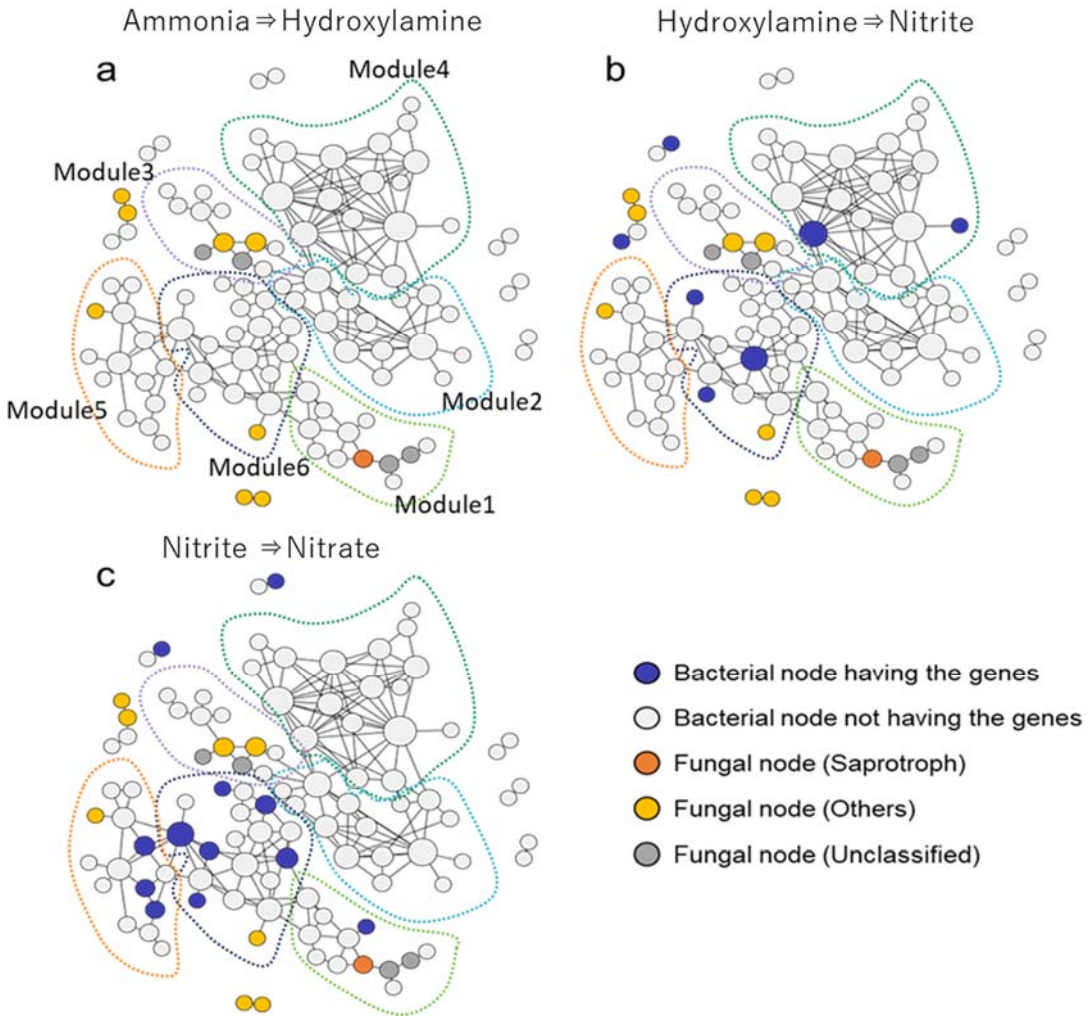

Fig. 8 Nakayama et al.